

The Structures of Cyclopropane–Amine van der Waals Complexes

Susan E. Forest and Robert L. Kuczkowski*

Contribution from the Department of Chemistry, University of Michigan, Ann Arbor, Michigan 48109-1055

Received August 18, 1995[⊗]

Abstract: The rotational spectra of the cyclopropane–trimethylamine (CYC·TMA) and cyclopropane–dimethylamine (CYC·DMA) complexes have been observed using a pulsed nozzle, Fourier transform microwave spectrometer. The spectrum of CYC·TMA is characteristic of a symmetric top, $B_0 = 1172.2800(1)$ MHz. Unlike the symmetric top complex of cyclopropane–ammonia (*Chem. Phys. Lett.* **1994**, *218*, 349–352), the CYC·TMA complex did not exhibit effects from internal rotation about the C_3 axis. The CYC·DMA complex has an asymmetric top spectrum with $A = 5095.137(9)$ MHz, $B = 1456.477(2)$ MHz, and $C = 1301.365(1)$ MHz. Both structures have the amine sitting above the ring, with the lone pair pointing toward the cyclopropane. A comprehensive discussion of the three cyclopropane–amine complexes in terms of spectral characteristics and constants, structure, strength, and dynamics is included, as well as an effort to understand the origin of these interactions from an examination of the electrostatic potential of cyclopropane. We also contrast the cyclopropane–base complexes with the cyclopropane–acid complexes found in the literature.

Introduction

Cyclopropane has unusual properties with respect to binding and reactivity when compared to other cycloalkanes. This prototype triangular shaped species undergoes certain reactions (for example, electrophilic addition of bromine) that are more analogous to ethylene and other olefin molecules than to typical cycloalkanes.¹

Two models that are often used to explain the characteristics of cyclopropane are the Coulson and Moffitt bent bond model² and the Walsh sp^2 hybridized orbital model.³ The Coulson and Moffitt model describes the C–C bonds of cyclopropane as “bent” since the maximum electron density is not along the C–C internuclear axis; rather, appreciable electron density is found off this axis, directed away from the ring. In addition to the electronic charge in the bent bonds, theoretical studies⁴ have shown that there is significant electron density spread out about the entire ring plane.

With this knowledge, chemists have used rotational spectroscopy to look at weak hydrogen-bonded complexes of cyclopropane (CYC), such as CYC·HF,⁵ CYC·HCl,⁶ CYC·H₂O,⁷ and CYC·HCN,⁸ in order to determine the structure of the complex and the mode of interaction. In each case, the complex exhibits an overall structure in which the HX subunit lies in the plane of the cyclopropane ring and is hydrogen bonded to the center of one of the equivalent C–C bonds. The results of these studies are consistent with the Coulson and Moffitt

description of cyclopropane since the HX hydrogen is attracted to the area of highest electron density of the ring (the bent bond).

Little work has been done on complexes of cyclopropane with non-hydrogen donor moieties. Recently, however, we found a new structure for cyclopropane complexes with the study of the cyclopropane–ammonia complex.⁹ The structure of CYC·NH₃ is stacked with the lone pair of the nitrogen atom pointing toward the center of the cyclopropane ring. The complex has a symmetric top spectrum with free or nearly free internal rotation of the ammonia subunit about the C_3 axis.

In light of this novel structure, we have investigated two more amine complexes, cyclopropane–trimethylamine (TMA) and cyclopropane–dimethylamine (DMA). TMA has a significantly larger proton affinity than ammonia ($PA_{TMA} = 221.6$ kcal/mol and $PA_{NH_3} = 202$ kcal/mol).¹⁰ The proton affinity of DMA (217.8 kcal/mol)¹⁰ falls between that of TMA and NH₃. Thus, any predominant structural and dynamical variations in this series could provide interesting information on the relationship of such energetic properties to the structures and stabilities of van der Waals complexes. In addition, DMA has an asymmetry absent in the symmetric top molecules of TMA and NH₃, so we are particularly interested to learn whether any structural changes occur in this complex compared to CYC·TMA and CYC·NH₃.

The purpose of this work is to understand how these prototype amines interact with cyclopropane, to evaluate how their complexes differ from hydrogen-bonded cyclopropane complexes, and to explore how the electronic charge distribution of cyclopropane may influence the formation of weakly bonded complexes.

Experimental Section

The rotational spectra of CYC·TMA and CYC·DMA were observed using a Balle-Flygare type Fourier transform microwave (FTMW)

(9) Forest, S. E.; Kuczkowski, R. L. *Chem. Phys. Lett.* **1994**, *218*, 349–352.

(10) Aue, D. H.; Webb, H. M.; Bowers, M. T. *J. Am. Chem. Soc.* **1976**, *98*, 311–317.

(11) (a) Hillig, K. W., II; Matos, J.; Scioly, A.; Kuczkowski, R. L. *Chem. Phys. Lett.* **1987**, *133*, 359–362. (b) Balle, T. J.; Flygare, W. H. *Rev. Sci. Instrum.* **1981**, *52*, 33–45.

[⊗] Abstract published in *Advance ACS Abstracts*, December 15, 1995.

(1) (a) Zabicky, J., Ed. *The Chemistry of Alkenes*; Interscience: London, 1970; Vol. 2, pp 511–610. (b) Bunker, R. J.; Peyerimhoff, S. D. *J. Phys. Chem.* **1969**, *73*, 1299.

(2) Coulson, C. A.; Moffitt, W. E. *Philos. Mag.* **1949**, *40*, 1–35.

(3) Walsh, A. D. *Trans. Faraday Soc.* **1949**, *45*, 179–190.

(4) (a) Cremer, D.; Kraka, E. *J. Am. Chem. Soc.* **1985**, *107*, 3800–3810. (b) Wiberg, K. B.; Bader, R. F. W.; Lau, C. D. H. *J. Am. Chem. Soc.* **1987**, *109*, 985–1001.

(5) Buxton, L. W.; Aldrich, P. D.; Shea, J. A.; Legon, A. C.; Flygare, W. H. *J. Chem. Phys.* **1981**, *75*, 2681–2686.

(6) Legon, A. C.; Aldrich, P. D.; Flygare, W. H. *J. Am. Chem. Soc.* **1982**, *104*, 1486–1490.

(7) Andrews, A. M.; Hillig, K. W., II; Kuczkowski, R. L. *J. Am. Chem. Soc.* **1992**, *114*, 6765–6770.

(8) Kukolich, S. G. *J. Chem. Phys.* **1983**, *78*, 4832–4835.

spectrometer equipped with a pulsed nozzle source.¹¹ Line widths were typically 30 kHz full width at half maximum with center frequencies estimated to be accurate to approximately ± 4 kHz. Stark effect measurements for the TMA complex were made by using two 50 cm \times 50 cm steel mesh grids, separated by a distance of 30 cm, placed above and below the cavity. The voltage applied to the grids can vary from 0 to 10 kV with opposite polarity. The electric field was calibrated by measuring the Stark shift of the $1 \leftarrow 0$ transition of OCS ($\mu = 0.715196$ D).¹²

The sample was composed of approximately 2% each of CYC and ¹⁴N-TMA (both obtained from Aldrich Chemical Co.) seeded in a 80:20 neon/helium carrier gas mix at a total pressure of 1–2 atm. The ¹⁵N-TMA (99 atom % ¹⁵N) sample was obtained from Isotech Isotope Laboratories in the form of the hydrochloride salt. The ¹⁵N-TMA was liberated from the salt by the addition of NaOH pellets and a few drops of 2 N NaOH solution. The evolving gas was passed through a trap held at -78 °C and collected in a liquid nitrogen trap.

A sample of similar composition was used in the CYC·DMA experiments. DMA was obtained from Linde. The ¹⁵N-DMA (99 atom % ¹⁵N) was also obtained from Isotech Isotope Laboratories as N(CH₃)₂H·HCl. It was liberated with basically the same procedure described above, although the DMA·HCl was more sensitive to the amount of NaOH used in the extraction; too much base would quench the liberation of DMA from its hydrochloride salt. The N(CH₃)₂D species was formed by allowing N(CH₃)₂H and D₂O to undergo proton exchange in a glass bulb. The water species were separated into a trap held at -78 °C and the N(CH₃)₂D gas was collected with a liquid nitrogen trap. In addition, extensive conditioning of the sample inlet line with D₂O was required to observe signals from this isotopomer. The *1,1-d*₂-CYC (98 atom % D) species was purchased from MDS Isotopes.

Results and Analysis

A. Spectral Assignment. i. Cyclopropane–Trimethylamine. The model used for the CYC·TMA complex was similar to the stacked symmetric top structure found for CYC·NH₃, but with a shorter interaction distance. Transitions (up to $J = 7$, $K = 5$) were observed and least-squares fits to the expression for a symmetric top,¹³ $\nu = 2B_0(J + 1) - 4D_J(J + 1)^3 - 2D_{JK}(J + 1)K^2$. The fits for both the CYC·¹⁴N-TMA species and the CYC·¹⁵N-TMA isotopomer are found in Table 1. The electric quadrupole coupling constant of the CYC·¹⁴N-TMA species was determined from a fit of the quadrupole-split components that arise from the coupling of the nuclear spin of the ¹⁴N nucleus with the molecular rotational angular momentum of the complex. The experimental value of the quadrupole coupling constant determined for the complex was $\chi_{aa} = -5.387(3)$ MHz. The fit of the quadrupole-split transitions can be found in Table S1. (See the paragraph at the end of the paper regarding supporting information.) The spectroscopic constants derived from the fit of center frequencies are listed in Table 2.

Stark effect measurements were made on the CYC·¹⁵N-TMA species. The $K \neq 0$ and $K = 0$ transitions demonstrated the first- and second-order Stark shift patterns, respectively, expected for a symmetric top. The second-order shifts of the 4_0-3_0 and 5_0-4_0 transitions were used to calculate the total dipole moment of the complex, $\mu = 1.00(2)$ D. As with the CYC·NH₃ spectrum, the CYC·TMA spectrum was initially very complicated to understand because of overlapping quadrupole components of different K states and was best understood after the assignment of the CYC·¹⁵N-TMA species. No additional transitions were found in the spectrum.

ii. Cyclopropane–Dimethylamine. The spectrum of cyclopropane–dimethylamine was discovered by again using a

Table 1. Center Transition Frequencies (ν_{obs}) for Cyclopropane–Trimethylamine

transition $J_K - J'_K$	CYC· ¹⁴ N-TMA		CYC· ¹⁵ N-TMA	
	$\nu_{\text{obs}}/\text{MHz}^a$	$\Delta\nu/\text{kHz}^b$	$\nu_{\text{obs}}/\text{MHz}$	$\Delta\nu/\text{kHz}^b$
3 ₀ -2 ₀	7033.539	0.3	7011.181	2.2
3 ₁ -2 ₁	7033.471	0.5	7011.111	0.0
3 ₂ -2 ₂	7033.266	-0.1		
4 ₀ -3 ₀	9377.906	0.7	9348.090	-2.8
4 ₁ -3 ₁	9377.813	-1.4	9348.002	-0.4
4 ₂ -3 ₂	9377.538	-3.8	9347.733	1.8
4 ₃ -3 ₃	9377.087	-0.3	9347.283	3.9
5 ₀ -4 ₀	11722.149	2.5	11684.881	-1.0
5 ₁ -4 ₁	11722.034	1.1	11684.768	-1.0
5 ₂ -4 ₂	11721.692	-0.1	11684.430	0.1
5 ₃ -4 ₃	11721.124	-0.1	11683.864	-0.9
5 ₄ -4 ₄			11683.073	-0.8
6 ₀ -5 ₀	14066.231	0.1	14021.515	-0.2
6 ₁ -5 ₁	14066.096	1.4	14021.380	0.4
6 ₂ -5 ₂	14065.685	-0.6	14020.970	-2.7
6 ₃ -5 ₃	14065.005	1.0	14020.293	-1.6
6 ₄ -5 ₄			14019.346	0.7
6 ₅ -5 ₅			14018.126	1.3
7 ₀ -6 ₀	16410.127	-0.3	16357.961	-0.2
7 ₁ -6 ₁	16409.967	-1.2	16357.806	3.0
7 ₂ -6 ₂	16409.490	-1.1	16357.328	-0.3
7 ₃ -6 ₃	16408.697	1.1	16356.539	1.8
7 ₄ -6 ₄			16355.428	-1.6
7 ₅ -6 ₅			16354.005	-0.6

^a For the ¹⁴N species, this is the center frequency in the absence of hyperfine splitting from the ¹⁴N nuclear electric quadrupole moment. The quadrupole-split transitions are provided in the supporting information. ^b $\Delta\nu = \nu_{\text{obs}} - \nu_{\text{calc}}$ where ν_{calc} is obtained from the rotational and distortion constants found in Table 2.

Table 2. Spectroscopic Constants for the Isotopic Species of Cyclopropane–Trimethylamine

constants	CYC· ¹⁴ N-TMA	CYC· ¹⁵ N-TMA
B_0/MHz	1172.2800(1)	1168.5532(1)
D_J/kHz	1.306(1)	1.300(1)
D_{JK}/kHz	11.360(9)	11.302(4)
χ_{aa}/MHz	-5.387(3)	
n^a	19	23
$\Delta\nu_{\text{rms}}/\text{kHz}^b$	1.3	1.7

^a Number of transitions in the fit. ^b $\Delta\nu_{\text{rms}} = \{(\sum(\nu_{\text{obs}} - \nu_{\text{calc}})^2)/n\}^{1/2}$.

stacked structural model. We assumed an interaction distance that was close to what was obtained for CYC·TMA. (R is denoted as the interaction distance, the distance from the center of mass (COM) of cyclopropane to the nitrogen atom.) Previous work on water–amine complexes^{14,15} suggested that the change in R would be small, on the order of 0.03 Å. The quantum numbers were assigned with the aid of the nuclear quadrupole splitting pattern. Unsplit center frequencies were fitted to the standard Watson S-reduced semirigid rotor Hamiltonian (I' representation). We observed a -type transitions and a couple of very weak c -types; no b -type transitions were detected despite accurate predictions based on the fitted a - and c -type transition frequencies. We also assigned the spectra of the CYC·¹⁵N-DMA, CYC·(CH₃)₂ND, and *1,1-d*₂-CYC·DMA species. Although there were extra transitions in the normal species, no additional transitions were observed in some of the corresponding $J + 1 \leftarrow J$ regions in the other isotopomers. Our attempts to identify quadrupole patterns and to assign these transitions as tunneling doublets proved unsuccessful. The fit of the center frequencies can be found in Table 3.

(12) Tanaka, K.; Ito, H.; Harada, K.; Tanaka, T. *J. Chem Phys.* **1984**, *80*, 5893–5905.

(13) Gordy, W.; Cook, R. L. *Microwave Molecular Spectra*; Wiley: New York, 1984; pp 175–182.

(14) Tubergen, M. J.; Kuczkowski, R. L. *J. Mol. Struct.* **1995**, *352/353*, 335–344.

(15) Tubergen, M. J.; Kuczkowski, R. L. *J. Am. Chem. Soc.* **1993**, *115*, 9263–9266.

Table 3. Center Transition Frequencies (ν_{obs}) for Cyclopropane–Dimethylamine Isotopomers

transition $J'_{K'_a K'_b} - J''_{K''_a K''_b}$	CYC·N(CH ₃) ₂ H		CYC· ¹⁵ N(CH ₃) ₂ H		CYC·N(CH ₃) ₂ D		<i>l,l</i> -d ₂ -CYC·N(CH ₃) ₂ H	
	$\nu_{\text{obs}}/\text{MHz}^a$	$\Delta\nu/\text{kHz}^b$	$\nu_{\text{obs}}/\text{MHz}^a$	$\Delta\nu/\text{kHz}^b$	$\nu_{\text{obs}}/\text{MHz}^a$	$\Delta\nu/\text{kHz}^b$	$\nu_{\text{obs}}/\text{MHz}^a$	$\Delta\nu/\text{kHz}^b$
3 ₁₃ –2 ₁₂	8037.550	0.1	7990.240	0.6	7953.730	3.0	7794.148	–2.7
3 ₀₃ –2 ₀₂	8253.885	0.5	8202.955	–0.5	8155.232	–6.9	8007.511	–4.3
3 ₂₂ –2 ₂₁	8272.914	1.6						
3 ₂₁ –2 ₂₀	8292.288	–6.3						
3 ₁₂ –2 ₁₁	8502.730	–6.4	8447.051	–0.1	8385.362	–0.5	8254.045	–1.0
5 ₀₅ –4 ₁₃	9141.579	–0.5						
4 ₁₄ –3 ₁₃	10711.047	0.6	10648.156	–1.0	10599.927	–4.4	10386.442	3.2
4 ₀₄ –3 ₀₃	10982.506	0.6	10915.380	3.9	10853.646	9.1	10653.615	5.7
4 ₁₃ –3 ₁₂	11330.796	0.2	11256.766	–0.1	11175.027	1.1	10999.107	1.7
3 ₁₂ –2 ₀₂	12456.377	–0.2						
5 ₁₅ –4 ₁₄	13379.949	1.1	13301.630	0.9	13242.054	1.8	12974.081	–0.9
5 ₀₅ –4 ₀₄	13692.366	4.0	13609.648	–5.0	13535.410	–3.2	13280.646	–2.1
5 ₁₄ –4 ₁₃	14153.273	9.0	14061.092	0.0	13959.769	–0.5	13738.471	–0.7
6 ₁₆ –5 ₁₅	16043.449	6.3	15949.864	–0.4				
6 ₀₆ –5 ₀₅	16380.159	–11.6	16282.569	1.8				
6 ₁₅ –5 ₁₄	16968.379	–1.7	16858.337	0.1				

^a For the ¹⁴N species, this is the center frequency in the absence of hyperfine splitting from the ¹⁴N nuclear electric quadrupole moment. The quadrupole-split transitions are provided in the supporting information. ^b $\Delta\nu = \nu_{\text{obs}} - \nu_{\text{calc}}$ where ν_{calc} is obtained from the rotational and distortion constants found in Table 4.

Table 4. Spectroscopic Constants for the Isotopic Species of Cyclopropane–Dimethylamine

	CYC·N(CH ₃) ₂ H	CYC· ¹⁵ N(CH ₃) ₂ H	CYC·N(CH ₃) ₂ D	<i>l,l</i> -d ₂ -CYC·N(CH ₃) ₂ H
<i>A</i> /MHz	5095.1372(89)	5082.4(2)	4994(1)	4899.5(8)
<i>B</i> /MHz	1456.4775(16)	1446.4790(8)	1434.055(3)	1414.596(2)
<i>C</i> /MHz	1301.3653(12)	1294.1614(7)	1290.133(3)	1261.244(2)
<i>D</i> _{<i>j</i>} /kHz	2.421(9)	2.345(8)	2.29(4)	2.21(3)
<i>D</i> _{<i>JK</i>} /kHz	14.7(2)	15.5(5)	17(2)	14(1)
<i>d</i> _{<i>j</i>} /kHz	–0.26(2)	–0.236(5)	–0.22(3)	–0.27(2)
χ_{aa} /MHz	–5.049(3)		–5.071(11)	–5.038(8)
χ_{bb} /MHz	2.924(4)		2.923(15)	2.936(21)
<i>P</i> _{bb}	70.273	70.278	70.258	73.293
<i>n</i> ^a	16	12	9	9
$\Delta\nu_{\text{rms}}$ /kHz ^b	4.7	2.0	4.4	2.9

^a Number of transitions in the fit. ^b $\Delta\nu_{\text{rms}} = \{(\sum(\nu_{\text{obs}} - \nu_{\text{calc}})^2)/n\}^{1/2}$.

The quadrupole coupling constants for the ¹⁴N nucleus in the CYC·¹⁴N-DMA, CYC·(CH₃)₂ND, and *l,l*-d₂-CYC·DMA species were determined from a least-squares fit of the quadrupole-split components (Tables S2 and S3). The line widths for the latter two species were on the order of 60–100 kHz wide (fwhm) on account of unresolved splittings due to deuterium quadrupole effects. The values for the quadrupole coupling constants and the other spectroscopic constants for the CYC·DMA complex are listed in Table 4.

B. Structure. i. Cyclopropane–Trimethylamine. CYC·TMA has a symmetric top spectrum. Hence, only one parameter, namely *R*, can be determined from the moments of inertia of the two isotopic species, assuming that the monomer structures of cyclopropane¹⁶ and trimethylamine¹⁷ are not perturbed upon complexation. Two structures were obtained using a least-squares procedure to determine *R* from the two isotopes. Structure **I** has the TMA above the cyclopropane molecule with the nitrogen atom pointing toward the ring; the interaction distance *R* (distance from N to the COM of the ring) for this structure is 3.4060(1) Å. Structure **II** is also a symmetric top with the TMA above the cyclopropane ring, but with the methyl groups pointing toward the ring. In this structure, *R* = 4.120(4) Å. The quality of the first fit was much better for the two isotopomers ($\Delta I_{\text{rms}} = 0.031 \text{ amu } \text{Å}^2$) than for the second ($\Delta I_{\text{rms}} = 1.14 \text{ amu } \text{Å}^2$). In essence, the nitrogen isotope shift data are only consistent with the nitrogen end of TMA being closer to cyclopropane than its methyl end. In addition, previous

Table 5. Structural Analysis of Cyclopropane–Trimethylamine

	structure I N lone pair toward ring	structure II N methyl groups toward ring
<i>R</i> (N-ring COM)/Å ^a	3.4060(1)	4.120(4)
nitrogen <i>a</i> -coord/Å ^b	1.206	1.923
$\Delta I_{\text{rms}}/\text{amu } \text{Å}^2$ ^c	0.031	1.138

^a COM is center of mass. ^b This is the value determined from the least-squares fitting of the moments of inertia for the two isotopes. The *a*-coordinate of the nitrogen atom from Kraitchman's equation (see ref 30) is 1.180 Å, confirming that structure **I** is preferred. ^c $\Delta I_{\text{rms}} = \{(\sum(I_{\text{obs}} - I_{\text{calc}})^2)/n\}^{1/2}$.

experience with weakly bound complexes indicates that an interaction distance of 4 Å or greater is unusually large, also making the value of 4.120 Å unreasonable.

These structural arguments (summarized in Table 5) led to the conclusion that the structure (averaged over zero-point motions, an *r_o* structure) of the CYC·TMA complex has the TMA sitting above the cyclopropane molecule with the nitrogen lone pair pointing toward the center of the ring. The small uncertainty in *R* listed in Table 5 is the statistical value from the least-squares fitting. It is not easy to quantitatively estimate the deviation of the *r_o* structure from that of the equilibrium structure *r_e*. Given the floppy nature of weakly bound complexes, vibrational effects could be sizable. An uncertainty in *R* of 0.03 Å is perhaps more realistic.

Some additional information on the deviations from a symmetric top symmetry arising from zero-point motion (denoted by the angle γ) can be obtained from the quadrupole coupling constant and is discussed below. The pictorial representation of the CYC·TMA complex can be found in Figure

(16) Endo, Y.; Chang, M. C.; Hirota, E. *J. Mol. Spectrosc.* **1987**, *126*, 63–71.

(17) Wollrab, J. E.; Laurie, V. W. *J. Chem. Phys.* **1969**, *51*, 1580–1583.

(18) Wollrab, J. E.; Laurie, V. W. *J. Chem. Phys.* **1968**, *48*, 5058–5066.

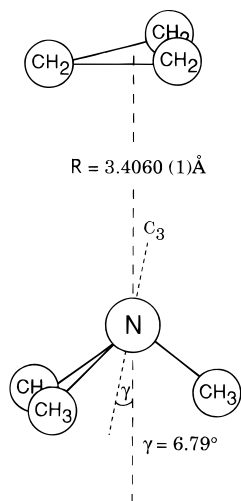


Figure 1. The structure of the cyclopropane–TMA complex. R is the separation between the nitrogen atom of the TMA and the center of mass of the cyclopropane ring. γ is the vibrationally-averaged bending angle formed between the C_3 axis of TMA and the a axis of the complex.

1. No information can be obtained from the spectrum on whether the methyl groups stagger or eclipse the cyclopropane CH_2 groups.

ii. Cyclopropane–Dimethylamine. Our data suggests that the structure for the $CYC \cdot DMA$ complex contains an ac plane of symmetry. Comparison of the planar moment ($P_{bb} = 0.5(I_a + I_c - I_b) = \sum m_i b_i^2$) for the normal species with those of the isotopic species $CYC \cdot ^{15}N$ -DMA and $CYC \cdot N(CH_3)_2D$ suggests that the substituted atoms lie in the ac symmetry plane of the complex (see Table 4) since their values for P_{bb} change only slightly when isotopic substitution occurs at those atom positions. Also, P_{bb} of the complex ($70.2733 \text{ amu } \text{Å}^2$) is nearly equal to the sum of the planar moments along the symmetry axes of free DMA ($P_{bb} = 50.4481 \text{ amu } \text{Å}^2$) and free CYC ($P_{bb} = 20.1254 \text{ amu } \text{Å}^2$), indicating that the symmetry planes of the individual monomers are contained within the symmetry plane of the complex. And lastly, b -type transitions were not observed.

Although P_{bb} of the normal species nearly equals the sum of the P_{bb} 's of the individual monomers, this is not sufficient to assure that an ac plane of symmetry exists in the complex. For the normal isotopic species, rotation of cyclopropane about its C_3 symmetry axis produces the same rotational constants and planar moments. Therefore, we cannot determine the position of one monomer relative to the other along that axis and cannot prove that the complex has a plane of symmetry based on this planar moment data alone. Instead, we need to compare the planar moment of the $1,1$ - d_2 - $CYC \cdot DMA$ species with the planar moment of the normal species. The $1,1$ - d_2 - $CYC \cdot DMA$ isotopomer breaks the symmetry of the cyclopropane ring, so now rotation about the C_3 axis will result in different values for the planar moments. A plot of ΔP_{bb} vs τ (Figure 2) represents how the difference (ΔP_{bb}) between P_{bb} of the normal species and the $1,1$ - d_2 - $CYC \cdot DMA$ species varies as cyclopropane rotates about its C_3 axis (rotation denoted by τ). As τ changes, the value of ΔP_{bb} oscillates as the CD_2 group rotates into and out of structures that contain a symmetry plane. The undeuterated complex only maintains an ac plane of symmetry when τ equals 0° , 60° , 120° , or 180° . These angles are indicated on the curve in Figure 2 by the open square data points. The dotted line with the diamonds represents the experimental ΔP_{bb} value. The experimental value of ΔP_{bb} nicely intersects with the positions on the curve that represent structures that contain an ac plane

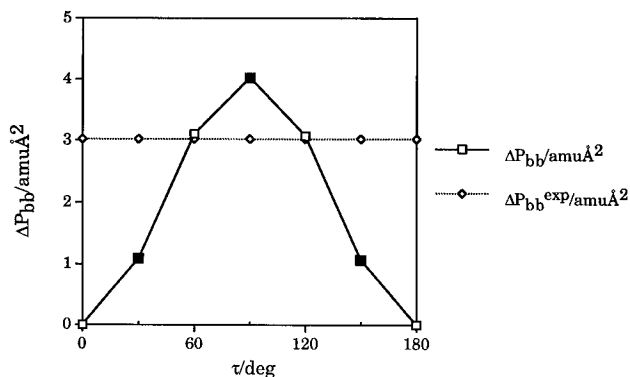


Figure 2. A plot of ΔP_{bb} vs τ . ΔP_{bb} is the difference between P_{bb} of the normal species and the $1,1$ - d_2 - $CYC \cdot DMA$ species. τ is the rotation angle of cyclopropane about its C_3 axis ($\tau = 0^\circ$ is defined in Figure 4). The solid curve (\square) represents the calculated ΔP_{bb} as τ varies from 0 to 180° ; the dotted curve (\diamond) represents the experimentally determined value of ΔP_{bb} .

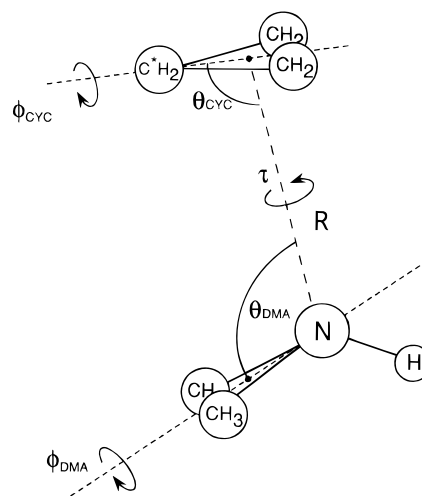


Figure 3. Structural parameters of the cyclopropane–dimethylamine complex. θ_{CVC} describes the tilt of the cyclopropane plane. θ_{DMA} is the tilt of the DMA. R is the distance from the nitrogen atom to the COM of the cyclopropane ring. ϕ_{CVC} and ϕ_{DMA} are the wagging angles of the cyclopropane ring and DMA monomers respectively; τ represents the torsional angle. The COM of each monomer is denoted by a dot (\bullet). ϕ_{CVC} , ϕ_{DMA} , and τ are the parameters that define an ac plane of symmetry (see text).

of symmetry. Therefore, the $1,1$ - d_2 - $CYC \cdot DMA$ isotopic data indicate that $CYC \cdot DMA$ has an ac plane of symmetry.

Assuming that the structures of the individual monomers of CYC^{16} and DMA^{18} do not change significantly upon complexation, we have least-squares fit I_{bb} and I_{cc} for all four observed species in order to obtain a structure for this complex. I_{aa} was not included in these structural fits because this value was not well determined for all the isotopes. Due to the decrease in intensity of the isotopic transitions, c -type lines were only assigned for the normal species. In addition, the out-of-plane tilts of the individual monomers affect I_{aa} more than they do I_{bb} or I_{cc} ; therefore, I_{aa} will be most contaminated by vibrational motions leading to less useful values. The structural parameters for this complex are described in Figure 3. θ_{CVC} describes the tilt of the cyclopropane plane, and is defined by the in-plane cyclopropane CH_2 carbon (denoted as C^*), the center of mass (COM) of cyclopropane, and the nitrogen atom ($\angle C^* - COM_{CVC} - N$). θ_{DMA} is the tilt of the DMA and is defined by $\angle COM_{DMA} - N - COM_{CVC}$. R is the distance from the nitrogen atom to the center of mass of the cyclopropane ring.

Table 6. Planar Structures for CYC·DMA Consistent with Experiment^a

	structure I DMA H eclipsing CH ₂	structure II DMA H eclipsing C–C
<i>R</i> /Å	3.440(7)	3.440(7)
θ_{CYC} /deg	83(1)	98(1)
θ_{DMA} /deg	121.1(9)	121.0(9)
ΔI_{rms} /amu Å ² ^b	0.124	0.119

^a See Figure 3 and text for description of parameters. ^b $\Delta I_{\text{rms}} = \{(\sum(I_{\text{obs}} - I_{\text{calc}})^2)/n\}^{1/2}$.

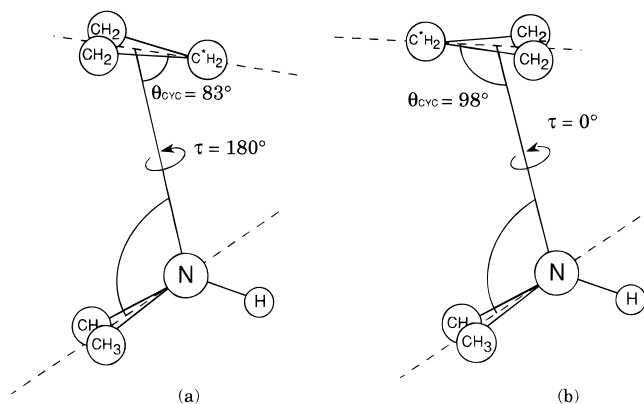


Figure 4. Conformers for cyclopropane–dimethylamine consistent with moments of inertia: (a) structure I. (b) structure II. Both figures have $R = 3.440 \text{ \AA}$ and $\theta_{\text{DMA}} = 121^\circ$.

When the dihedral angles that determine planarity are fixed to produce an *ac* plane of symmetry, namely $\phi_{\text{CYC}} = 90 \pm 180^\circ$, $\phi_{\text{DMA}} = 180^\circ \pm 180^\circ$, and $\tau = 0^\circ \pm 60^\circ$, the fitting produces two structures whose difference can be essentially described as a 180° rotation about τ , the torsional angle between the two monomers about R . Structure I has the DMA hydrogen atom eclipsing the cyclopropane CH₂ group, while structure II has the DMA hydrogen eclipsing a C–C ring bond. These differences can be seen in Table 6 and Figure 4. Another way of describing this is by noticing that in structure I, the in-plane C*H₂ group is above the DMA hydrogen atom, while in the other structure, the unique carbon is positioned over the methyl groups of DMA.

It is not possible to experimentally discriminate between these two structures. To do so would require better knowledge of the positions of all the atoms in the cyclopropane ring. We have made predictions of the rotational constants for the other *1,1-d₂*-CYC·DMA species and the ¹³C species and find that the isotope shift differences for the various species are not great enough to unambiguously distinguish between the two structures.

If we allow the angles that determine planarity (ϕ_{CYC} , ϕ_{DMA} , and τ) to vary in the least-squares fitting of the moments of inertia and do not rigidly fix an *ac* plane of symmetry, we find four structures that will fit the data. In these structures, ϕ_{DMA} and τ vary from the plane of symmetry values by at most $\sim 5^\circ$, while ϕ_{CYC} varies up to $\pm 15^\circ$. R becomes 3.46 \AA (different from 3.44 \AA in the symmetry plane fits), and θ_{DMA} converges to about 118° (different from 121° in the *ac* plane fits). The only angle that takes on distinctly different values in these fits is θ_{CYC} , and this allows for many possible orientations of the cyclopropane; the C*H₂ can be tilted toward or away from the amine (giving two structures) and then either eclipsing the DMA hydrogen or staggering the methyl groups (same ambiguity found in the structures with an *ac* plane), resulting in four conformations. The quality, as determined by ΔI_{rms} , was slightly better with the non *ac* plane fits than with a rigid plane of

symmetry. These small deviations from a symmetry plane can be discussed in terms of vibrational motions of the molecules that affect the moments of inertia by up to a few percent. Although these asymmetric structures cannot be rigorously eliminated, vibrational averaging effects are the likely origin of such results. In the absence of any more compelling evidence for the less symmetric structures, we will assume in the remainder of the discussion that one of the two symmetric forms (found in Figure 4) is the correct structural model.

Since the moments of inertia were fit directly, without corrections for large-amplitude vibrational motions, the uncertainties in the structural parameters given in Table 6 are not a true measure of the uncertainties in those parameters, but rather are the result of the statistical analysis of the least-squares fitting routine. Because of the floppy nature of weakly bound complexes, it is difficult to estimate how the observed vibrationally averaged moments of inertia are related to an equilibrium geometry. Therefore, it might be a more realistic estimate of the error in the structural parameters to say that R and θ should be within 0.05 \AA and 5° , respectively, of their equilibrium values.

C. Quadrupole Analysis. i. Cyclopropane–Trimethylamine. The ¹⁴N quadrupole coupling constant of free TMA ($\chi_o = -5.5024(25) \text{ MHz}$)¹⁹ has changed only a small amount upon complexation with cyclopropane ($\chi_{\text{aa}} = -5.387(3) \text{ MHz}$). We can use this value to estimate the zero-point bending amplitude of the TMA monomer in the complex, assuming that complexation does not affect the electronic structure at the nitrogen atom. This value is represented by γ , the vibrationally-averaged bending angle, which is the angle between the *a* axis of the complex and the symmetry axis of TMA. Using the expression $\chi_{\text{aa}} = \chi_o^{1/2}(3 \cos^2 \gamma - 1)$, γ is determined to be 6.79° .

ii. Cyclopropane–Dimethylamine. In order to make a comparison between the ¹⁴N quadrupole coupling constants in free DMA and those obtained from the complex, it is necessary to project and rotate the principal quadrupole axis of the monomer into the complex's principal axis system. It is apparent that the coupling constants of DMA have not changed markedly upon complexation. However, this calculation is not considered to be very accurate, as the values of the coupling constants for the nitrogen in free DMA are only good to $\pm 0.4 \text{ MHz}$.¹⁸ It is also more difficult to discuss a vibrationally-averaged bending angle for this complex since CYC·DMA is asymmetric, unlike the CYC·NH₃ and CYC·TMA complexes. Because of these problems, we do not feel it is worthwhile to make a quantitative comparison of the coupling constants in the free amine and the complex.

Discussion

A. Electrostatic Calculations. It has been apparent for some time that the electrostatic potential around a molecule can be a valuable probe of its chemical and physical properties.²⁰ Kollman and others²¹ have recognized that the electrostatic potential is a very useful guide to understanding non-covalent interactions. In addition, Ghio and Tomasi²² have shown that

(19) Rego, C. A.; Batten, R. C.; Legon, A. C. *J. Chem. Phys.* **1988**, *89*, 696–702.

(20) Politzer, P.; Truhlar, D. G., Eds. *Chemical Applications of Atomic and Molecular Electrostatic Potentials: Reactivity, Structure, Scattering, and Energetics of Organic, Inorganic, and Biological Systems*; Plenum Press: New York, 1981.

(21) (a) Kollman, P.; McKelvey, J.; Johansson, A.; Rothenberg, S. *J. Am. Chem. Soc.* **1975**, *97*, 955–965. (b) Kollman, P. *J. Am. Chem. Soc.* **1977**, *99*, 4875–4894. (c) Kollman, P. *Acc. Chem. Res.* **1977**, *10*, 365–371. (d) Scrocco, E.; Tomasi, J. *Adv. Quantum Chem.* **1978**, *11*, 115–193.

(22) Ghio, C.; Tomasi, J. *Theor. Chim. Acta* **1973**, *30*, 151–158.

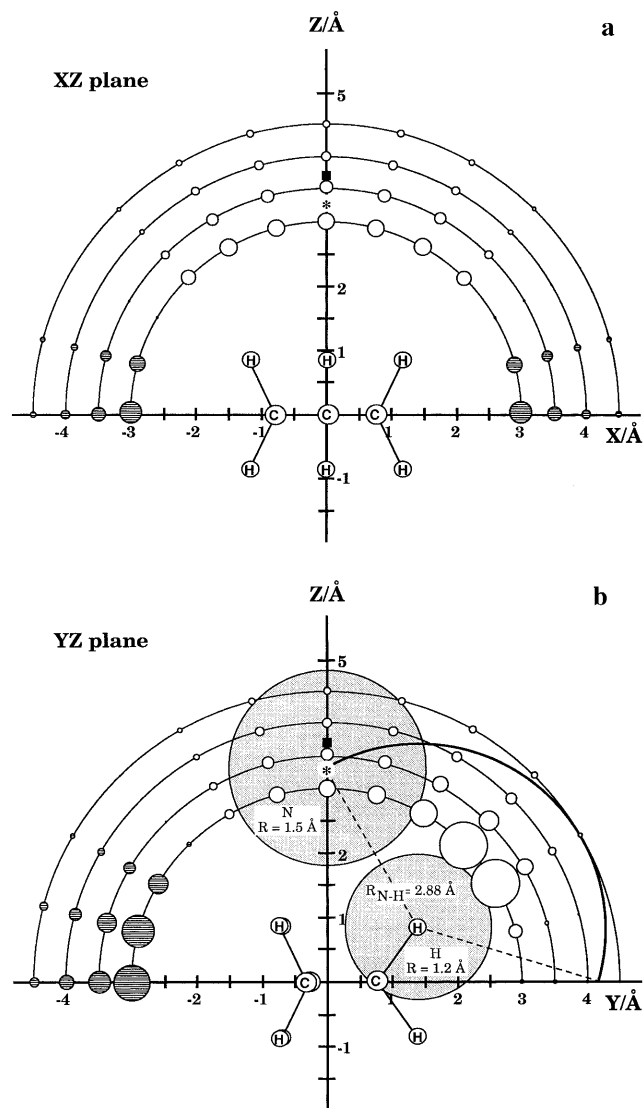


Figure 5. Maps of the electrostatic potential around cyclopropane. (a) XZ plane. Open circles indicate a positive electrostatic potential; striped circles indicate a negative potential. The relative magnitude of the potential is indicated by the size of the circle. Values are calculated at $R = 3.0, 3.5, 4.0,$ and 4.5 \AA as measured from the center of mass of the ring, at 15° increments. The black square indicates the position of the nitrogen atom in the complex with NH_3 ; the asterisk identifies the position of the nitrogen atom in the TMA complex. (b) YZ plane (see above). In addition, the large shaded circles represent the van der Waals radii of the nitrogen and hydrogen atoms. The value of the potential at $Y = -3.0 \text{ \AA}$ and $Z = 0 \text{ \AA}$ is -0.0111 au .

an electrostatic potential picture can be used to obtain an ordering of proton affinities, as well as information about protonation pathways and protonation sites of three-membered-ring compounds. We have examined the cyclopropane–amine complexes using this approach to provide a qualitative understanding of why the amines sit over the center of the ring.

Using Gaussian90,²³ the electrostatic potential of cyclopropane was calculated at many positions in the ring plane and around the cyclopropane molecule using the 6-31G** basis set. The potential in the XZ and YZ planes of cyclopropane can be observed in Figures 5a and 5b, respectively. In these figures, open circles designate points of positive electrostatic potential

while striped circles denote negative potential. The size of the circle represents the relative magnitude of the potential at that point. The black square indicates the location of the nitrogen atom in the ammonia complex (3.59 \AA above the ring plane), while the asterisk marks the position of the nitrogen atom in the TMA complex (3.41 \AA).

After study of Figure 5a, it seems reasonable that the lone pair of the nitrogen sits above the ring, on the Z axis, as this is the region of maximum positive potential. Slight zero-point motions rock the amine about this axis, but on average, the lone pair is stabilized by the large positive potential found above the ring. Figure 5b, however, is a bit more complicated; the region of largest positive potential is not located on the Z axis, but rather is $45\text{--}60^\circ$ off the Z axis. The question then becomes, why does the amine not interact at this more positive region, over a single hydrogen atom of the ring? To explain this, it is necessary to look at the van der Waals radii of the nitrogen and hydrogen atoms. The large shaded circles in Figure 5b represent the van der Waals radii of those atoms, with the nitrogen $R_{\text{vdw}} = 1.5 \text{ \AA}$ and hydrogen $R_{\text{vdw}} = 1.2 \text{ \AA}$. If an arc is mapped out by rotating a circle with a radius equal to the R_{vdw} of nitrogen about a circle with a radius equal to the R_{vdw} of hydrogen, it becomes apparent that the regions of highest positive potential are too close to the hydrogen atom for the nitrogen atom to penetrate without bumping of the van der Waals radii. Along this arc, the position of largest positive potential is then found on the Z axis, directly above the center of the cyclopropane ring where there is no overlap of the van der Waals radii. This qualitative (and crude) picture of the attractive and repulsive interactions serves to rationalize the general symmetry and structure of the complex.

It is also worth noting the regions of negative potential (striped circles) on the X and Y axes of these figures. The large accumulations of negative charge found at the center of the C–C bent bonds explains why a hydrogen donor forms its hydrogen bond with the C–C bond of the ring, as in the $\text{CYC}\cdot\text{HX}^{5-8}$ complexes previously studied.

In order to test the experimental results more quantitatively, electrostatic energy calculations were performed for both $\text{CYC}\cdot\text{TMA}$ and $\text{CYC}\cdot\text{DMA}$. We examined conformations for both complexes in which the methyl groups of the amine were staggered and eclipsed with respect to the CH_2 groups of cyclopropane. We employed the electrostatic interaction model of Buckingham and Fowler,²⁴ which requires a distributed multipole analysis²⁵ (DMA) of each subunit in the complex. The distributed multipoles moments for the monomers were calculated with a 6-31G** basis set using the DMA subroutines of the CADPAC program²⁶ and can be found in the supporting information as Tables S4 and S5. Previous studies²⁷ have shown that the Buckingham and Fowler model produces reasonable results for the geometries of many simple weak complexes even though it does not include an accurate repulsive term, or inductive and dispersion terms. We also have found that this

(24) Buckingham, A. D.; Fowler, P. W. *Can. J. Chem.* **1985**, *63*, 2018–2025.

(25) (a) Stone, A. J. *Chem. Phys. Lett.* **1981**, *83*, 233–239. (b) Price, S. L.; Stone, A. J.; Alderton, M. *Mol. Phys.* **1984**, *52*, 987–1001.

(26) Amos, R. D.; Rice, J. E. *Cambridge Analytic Derivatives Package (CADPAC)*; Issue 5.0, Cambridge, UK, 1992.

(27) (a) Andrews, A. M.; Taleb-Bendiab, A.; LaBarge, M. S.; Hillig, K. W., II; Kuczkowski, R. L. *J. Chem. Phys.* **1990**, *93*, 7030–7040. (b) Taleb-Bendiab, A.; Hillig, K. W., II; Kuczkowski, R. L. *J. Chem. Phys.* **1991**, *94*, 6956–6963. (c) Andrews, A. M.; Hillig, K. W., II; Kuczkowski, R. L.; Legon, A. C.; Howard, N. W. *J. Chem. Phys.* **1991**, *94*, 6947–6955. (d) Oh, J. J.; Hillig, K. W., II; Kuczkowski, R. L. *J. Am. Chem. Soc.* **1991**, *113*, 7480–7484. (e) Oh, J. J.; Xu, L.-W.; Taleb-Bendiab, A.; Hillig, K. W., II; Kuczkowski, R. L. *J. Mol. Spectrosc.* **1992**, *153*, 497–510.

(23) Gaussian90, Revision I; Frisch, M. J.; Head-Gordon, M.; Trucks, G. W.; Foresman, J. B.; Schlegel, H. B.; Raghavachari, K.; Robb, M.; Binkley, J. S.; Gonzalez, C.; Defrees, D. J.; Fox, D. J.; Whiteside, R. A.; Seeger, R.; Melius, C. F.; Baker, J.; Martin, R. L.; Kahn, L. R.; Stewart, J. J. P.; Topiol, S.; Pople, J. A. Gaussian, Inc.: Pittsburg, PA, 1990.

Table 7. Comparison of Amine Complexes with Cyclopropane and Water

	cyclopropane–amine complexes		
	CYC·NH ₃ ^a	CYC·DMA	CYC·TMA
PA ^b	202	217.8	221.6
D _J /kHz	16.61	2.421	1.306
D _{JK} /kHz	322.7	14.7	11.360
R/Å	3.592	3.439	3.406
k _s /Nm ⁻¹	3.64	6.18	7.95
ε/kcal·mol	0.97	1.46	1.84
	water–amine complexes ^c		
	H ₂ O·NH ₃	H ₂ O·DMA	H ₂ O·TMA
R/Å ^d	2.98	2.85	2.82

^a Values obtained from ref 9. ^b PA is the proton affinity of the free amine monomer in units of kcal/mol obtained from ref 10. ^c Values obtained from ref 14. ^d R is the heavy atom distance, R_{N-O}.

model is helpful in understanding the structures of many SO₂ complexes.²⁷

The binding energies obtained from the Buckingham and Fowler electrostatic energy calculations for the cyclopropane–amine complexes were generally at least an order of magnitude smaller (~100–500 cal/mol) than what is usually obtained from these electrostatic energy calculations (~1–3 kcal/mol) for weakly bound complexes. We have not been able to use calculations based on this model to make any meaningful conclusions about the structures and strengths of the cyclopropane–amine complexes or to reliably suggest which of the two CYC·DMA conformations (Figure 4) may be more stable.²⁸ Thus, at this time, the Buckingham and Fowler model seems less helpful in an analysis of these cyclopropane complexes. Although the electrostatic energy calculations do not help to determine a preferred structure of the cyclopropane–amine complexes, higher level *ab initio* calculations might be fruitful in this endeavor; such calculations, however, are beyond the scope of this paper.

B. Comparison to Other Complexes. It is appropriate to compare the CYC·TMA and CYC·DMA systems not only to each other, but to CYC·NH₃⁹ as well. As we stated in the introduction, we would like to compare the experimental results of structure, strength, and internal rotation effects of these complexes to what chemical intuition suggests the trends should be based on the proton affinities of these amine monomers. As we have seen from our electrostatic potential calculations about cyclopropane, these interactions seem to be lone pair–hydrogen in nature, validating the use of amine monomer proton affinity values as an intuitive chemical tool to base our comparisons. Table 7 summarizes some of the numbers that will be discussed in this section.

Structurally, all the amine moieties sit above the cyclopropane with the lone pair of the nitrogen pointing toward the ring. For the TMA and NH₃ complexes, this results in a symmetric top spectrum and structure. An asymmetric spectrum and stacked structure is obtained for CYC·DMA. CYC·TMA has the shortest N–ring COM distance of all the complexes; this is in agreement with the comparatively large proton affinity value of TMA. If TMA has a greater attraction for a hydrogen atom(s) than either DMA or NH₃, then we expect CYC·TMA to have the shortest interaction distance and CYC·NH₃ to have the longest R, with the value for the CYC·DMA complex falling somewhere in between. This pattern is found experimentally.

(28) It may be of interest to the reader that ΔE_{elec} of the CYC·DMA was 0.149 kcal/mol as determined from the Buckingham and Fowler calculation in favor of structure **I**. Structure **I** has the DMA hydrogen eclipsing a cyclopropane CH₂ group (see Figure 4).

In fact, the shortening of the interaction distance among the three cyclopropane complexes parallels the magnitude of that same reduction in the water–amine complexes¹⁴ (see Table 7). ΔR between the water complexes of DMA and TMA is about 0.03 Å, which is the same value for ΔR between CYC·DMA and CYC·TMA (0.033 Å). The ΔR between the NH₃ and DMA complexes of water and those for cyclopropane are also similar (0.130 Å for the water complexes and 0.153 Å for the cyclopropane complexes).

It is interesting that for either of the two *ac* plane of symmetry structures of the CYC·DMA complex, there is not a pronounced distortion of the pseudo-C₃ symmetric structure. In other words, the asymmetry of DMA has not caused the structure to deviate significantly from the structures of the other cyclopropane–amine complexes. The interactions between the DMA methyl groups or the DMA hydrogen and the cyclopropane ring are not considerably different (from those interactions in the CYC·NH₃ or CYC·TMA complexes) to cause a perturbation away from a near C₃ symmetric form.

Often times, the size of the interaction distance is inversely related to the strength of the complex. In order to obtain another relative measure of the strength of these three interactions, the pseudodiatomic model was employed. Assuming that the only van der Waals vibrational mode contributing to the D_J distortion constant is the stretching motion between the amine and cyclopropane, we can estimate a stretching force constant, k_s. This results in force constants of 7.95 and 6.18 N m⁻¹, which when used with a Lennard-Jones 6–12 potential yields binding energies of ε ≈ 1.84 and 1.46 kcal/mol for CYC·TMA and CYC·DMA, respectively. For the CYC·NH₃ complex, these values are much smaller (see Table 7). The results from this simple model rank the strengths of the cyclopropane–amine complexes from weakest to strongest as CYC·NH₃, CYC·DMA, and CYC·TMA. If we use the same method to calculate the ε of the CYC·HX complexes (X = Cl, F, CN, OH), we obtain a range of binding energies from 1.54 to 2.37 kcal/mol. The amine complexes fall on the low side of this range, possibly suggesting that the CYC–acid complexes (which lead to an acid hydrogen donor interaction with the C–C bond of the ring) are stronger than the CYC–base complexes, in which the roles of hydrogen donor/acceptor have been reversed. However, the assumptions in the model preclude any firm conclusions on the interaction strength.

The quadrupole coupling constants can give information about the rigidity of the complex and the electronic effects of complexation. The value of χ_{aa} for ¹⁴N in CYC·TMA only differs from that in free TMA by about 115 kHz. The value for γ (approximately 7°) in the CYC·TMA complex is significantly smaller than what was determined for the corresponding angle (30.51°)⁹ in the CYC·NH₃ complex, where the ¹⁴N coupling constant in free ammonia and in the complex differed by more than 1.5 MHz. We would expect that the most significant distortion of the electronic environment of the nitrogen nucleus due to complexation (as observed by a large Δχ, the difference between the quadrupole coupling constant in the free monomer to the value obtained in the complex) would be found in the CYC·TMA complex since that complex has the strongest interaction and the shortest R. However, the small Δχ in CYC·TMA (and CYC·DMA) implies that the complex has small polarization effects.

In addition, the only complex for which we definitively observe the presence of internal rotation effects about the nitrogen–CYC axis is for CYC·NH₃. No additional transitions from free or nearly free internal rotation were observed in CYC·TMA, and although we cannot completely rule out the

possibility of internal rotation in $\text{CYC}\cdot\text{DMA}$, we do not believe the unassigned transitions arise from tunneling splittings. Since ammonia is the farthest from the cyclopropane and the lightest amine, the prominence of tunneling effects is not considered unusual.

Conclusion

Cremer *et al.*⁴ have shown that cyclopropane has significant electron density spread over the ring. While this electron density is important in understanding the covalent interactions in cyclopropane, it is less pertinent to understanding the cyclopropane–amine complexes. The amine is located several angstroms (~ 3.5 Å) above the ring plane, making the interaction of the lone pair with the positive potential of the out-of-plane ring hydrogens the dominant interaction. On the other hand, the in-plane electron density between the carbons (bent bonds) does influence the electrostatic potential in the direction of proton approach and rationalizes the $\text{CYC}\cdot\text{HX}$ complexes.

The proton affinities¹⁰ of TMA and ammonia, as well as the evidence in the literature on $\text{TMA}\cdot\text{HX}$ ²⁹ complexes and $\text{TMA}\cdot\text{HOH}$,¹⁵ suggests that TMA forms stronger interactions than those of ammonia. We have shown that interactions with cyclopropane, acting as a proton donor with amines, are also consistent with these results. Our data imply that the order of

binding strength is $\text{CYC}\cdot\text{NH}_3 < \text{CYC}\cdot\text{DMA} < \text{CYC}\cdot\text{TMA}$. These results agree with chemical intuition as well as the proton affinities of the amine monomers.

In addition, we have shown that there is a change in structural type for $\text{CYC}\cdot\text{acid}$ versus $\text{CYC}\cdot\text{base}$ complexes. This contrast is reasonable when explored from the perspective of simple attractive and repulsion forces derived from examining the electrostatic potential obtained from HF *ab initio* calculations and consideration of van der Waals hard spheres.

Acknowledgment. This work has been supported by the National Science Foundation and a predoctoral fellowship to SEF from the University of Michigan Graduate School. The allotment of computer time for calculations at the San Diego Supercomputer is gratefully acknowledged.

Supporting Information Available: Tables S1–S5 listing the quadrupole-split frequency components of the $\text{CYC}\cdot\text{TMA}$ and $\text{CYC}\cdot\text{DMA}$ isotomers and the distributed multipoles for the two complexes (5 pages). This material is contained in libraries on microfiche, immediately follows this article in the microfilm version of the journal, can be ordered from the ACS, and can be downloaded from the Internet; see any current masthead page for ordering information and Internet access instructions.

JA952849Z

(29) (a) Legon, A. C.; Rego, C. A. *Chem. Phys. Lett.* **1989**, *162*, 369–375. (b) Legon, A. C.; Rego, C. A. *J. Chem. Phys.* **1989**, *90*, 6867–6876. (c) Legon, A. C.; Wallwork, A. L.; Rego, C. A. *J. Chem. Phys.* **1990**, *92*, 6397–6407.

(30) Kraitchman, J. *Am. J. Phys.* **1953**, *21*, 17–24.